Thermal performance of a box type solar cooker using artificial neural network

E.H. Amer
Mechanical Power Eng. Dept., Faculty of Eng., Shebin El-Kom, Menoufia University, Menoufia, Egypt
Email: amer_h_emad@yahoo.com

The objective of this study is to predict the thermal performance parameters of a box type solar cooker by using Artificial Neural Network (ANN). The parameters used to describe the thermal performance are the absorber plate temperature, the enclosure air temperature and the pot water temperature. For this purpose, a box type solar cooker was constructed and tested for its thermal performance under various experimental conditions. Solar radiation intensity, ambient, absorber plate, enclosure air and pot water temperatures were measured as a function of time. A feed-forward neural network based on back propagation algorithm was developed to predict the thermal performance of the solar cooker with and without reflectors. The experimental data set was divided into two groups. The first group, containing 75% of the data, was used for training/learning of the network. The second group, containing the rest of the data, was used for testing/validation of the network performance. The performance of the ANN predictions was evaluated by comparing the predicted results with experimental measurements. The results showed good regression analysis with correlation coefficients in the range of 0.9823-0.9982 and mean relative errors in the range of 4.516-6.751% for the test data set. The regression coefficients indicated that the ANN model can accurately be used for predicting the thermal performance parameters of the box type solar cooker.

يقدم البحث دراسة للتنبؤ بمتغيرات جهاز الطهى بالطاقة الشمسية نوع الصندوق بإستخدام الشبكة العصبية الإصطناعية. فى هذا البحث، تم تكوين نموذج رياضى بإستخدام شبكة عصبية ذات تغذية أمامية و تغذية عكسية راجعة لحساب متغيرات جهاز الطهى الشمسى. أختيرت درجات حرارة كل من لوح الإمتصاص و الهواء الداخلى و المياة كمتغيرات لوصف أداء جهاز الطهى. تم تصنيع جهاز طهى وإختباره فى مدى واسع لظروف التشغيل فى حالة إستخدام عواكس الإشعاع المستوية وفى حالة عدم إستخدام العواكس. قسمت البيانات المسجلة عمليا إلى مجموعتين، الأولى تضم ٧٥% من القياسات و إستخدمت لمعايرة الشبكة العصبية وتحديد معاملاتها، فى حين ضمت المجموعة الثانية ٢٥% من البيانات وتم إستخدامها فى إختبار و تحقيق أداء الشبكة. تم مقارنة النتائج النظرية المحسوبة بواسطة الشبكة العصبية مع القياسات العملية وأيضا مع النماذج الرياضية المتاحة من الأبحاث السابقة وأظهرت المقارنات توافقا مرضيا.

Keywords: Box type solar cooker, Thermal performance, Artificial neural network

1. Introduction

Solar cookers have attracted the attention of many researchers. Different types of solar cookers have been developed and tested all over the world. There has been a considerable recent interest in the design, development and testing of various types of solar cookers. Solar cookers can be classified mainly into three types; namely; box type, concentrating type and oven type. The box type solar cooker is commonly used for cooking at or around solar noon. It is the most popular type of cookers because it is cheaper and simpler to construct and operate than other types. A temperature above 100 °C can be achieved in such a cooker which makes it suitable for boiling type cooking. Several modifications have been introduced to the design of box type cookers in order to improve its performance. The modifications include fixing the cooking vessel to the absorber plate [1], introducing a heat storage element [2] and exposing the absorber from two sides to the incoming solar radiation [3].

The performance of box type solar cooker has been extensively investigated and many test procedures have been developed for thermal performance evaluation and prediction. Binark and Turkmen [4] have modeled the cooker by using the fourth order Runge-Kutta method. El-Sebaii [5] has

presented a simple model for a box type cooker with outer-inner reflectors. The model is based on analytical solution of the energy balance equations for different elements of the cooker. The performance is investigated in terms of the cooker efficiency. Kumar [6] has presented a simple test procedure for determination of design parameters to predict the thermal performance of the cooker. Mullick et. al. [7] have tested a box type cooker and obtained the second figure of merit F_2 and its variation with load and number of pots. Funk and Larson [8] have proposed a parametric model based on prediction of the cooking power of a solar cooker in terms of three controlled variables (solar intercept area, overall heat loss coefficient and absorber plate thermal conductivity) and three uncontrolled variables (insolation, temperature difference and load distribution). They concluded that the proposed model is valid for family size solar cookers. El-Sebaii and Ibrahim [9] have investigated the cooker performance by obtaining the two figures of merits F_1 and F_2 from experimental data. It has been reported that the best performance can be obtained with the maximum load in the cooker. Ekechukwu and Ugwuoke [10] have predicted the water boiling times using the two figures of merits and compared the results with measured values.

The objective of this study is to develop an Artificial Neural Network (ANN) model that can predict the thermal performance of a box type solar cooker based on some experimentally measured variables. Using this model, the thermal performance parameters such as absorber plate temperature (T_p), enclosure air temperature (T_a), and pot water temperature (T_w) have been predicted and compared with experimentally measured values. ANN has been successfully applied for modeling and prediction in many engineering systems. It has become increasingly popular in the last decade. Some of the recent applications in engineering systems include thermal engineering [11], mechanical and materials science [12], food and chemical process engineering [13]. Application of neural networks in thermal engineering can efficiently be extended to include various subjects such as; solar radiation estimation, thermal load prediction, cooling energy consumption, estimation of the heat transfer coefficient, and analysis of heat exchangers and HVAC systems.

2. Description of the solar cooker

The conventional box type solar cooker used for experimentation is constructed from materials commercially available in the markets. The cooker is single glazed with metal absorber. The body of the cooker is a double walled cylinder made of metal sheet of 38 cm inner diameter, 42 cm outer diameter and 25 cm height as shown schematically in fig. 1. Commercially available 1 mm thick copper plate is used as the absorber plate. It is painted matt black to improve its absorptivity. The gap between outer and inner walls of the cooker is filled with glass wool thermal insulation to minimize the heat losses. The inner surface is covered with aluminum foil to reflect the incident solar radiation on the base of absorber plate. The glazing material is 2 mm thick tempered glass which satisfies the cover desirable properties of high optical transmittance, low reflectivity and absorptance for solar radiation. The cooker is provided with a door of a rectangular shape of dimension 20×15 cm located at the center of the side wall. The cooking vessel is made of black painted aluminum pot of cylindrical shape having 16 cm diameter and 8 cm depth. It has a flat base to ensure a good thermal contact with the absorber plate. It is placed inside the cooker at the center of the absorber plate. The corners and edges of the cooker are well covered with silicon sealant to prevent any air leakage or infiltration.

Three plane reflectors are used to enhance the amount of radiation received by the cooker. The reflecting mirrors are fixed on a suitable iron framework in the west, east and north sides of the cooker with the tilt angle of 70°C to cooker side wall. This angle is chosen based on calculations following the procedure described in [14] such that the amount of radiation reflected on the absorber plate is maximized during the period of experimentations, while at the same time the

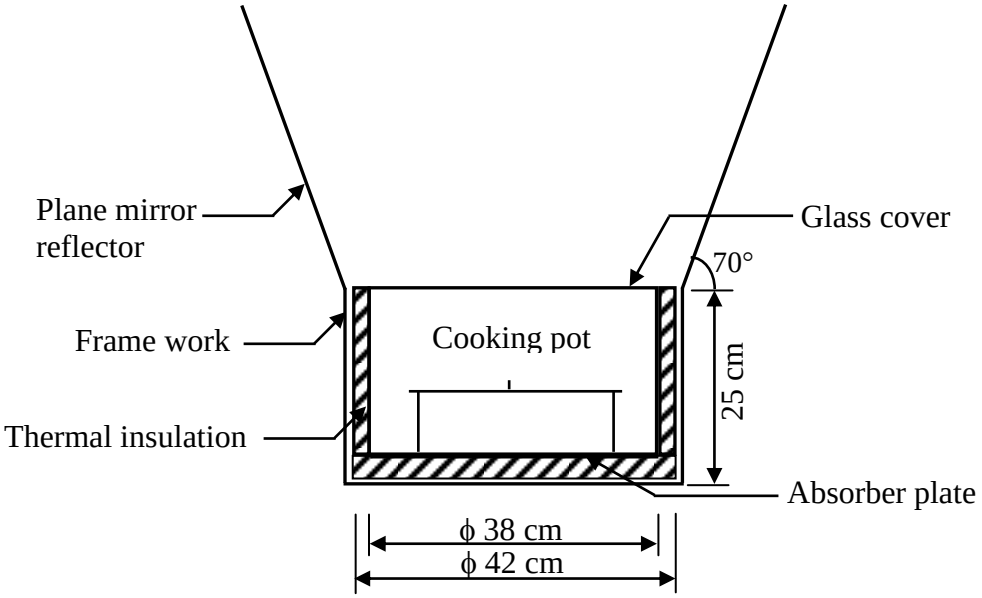

Fig. 1. Schematic diagram of the box type solar cooker.

shading effect is minimized. The plane reflectors are made of commercially available mirror of high optical reflectivity (ranging between 94 and 96%).

3. Experimental study

The constructed cooker was tested under the prevailing weather conditions of Shebin El-kom, Egypt (30.33 °N, 31.0° E). A series of experiments have been carried out on the cooker with and without the reflectors during the summer of 2005. Experiments have been conducted using three different quantities of water in the cooking pot with and without reflector respectively. The cooker has been loaded by 0.25 liter of water in the first experiment. The amount of water has been increased to 0.5 and 1 liter in the second and third experiments respectively. All experiments have been carried out within a range of 0 to 30° for the incidence angle of solar radiation. Experiments using reflectors have been conducted in the day following conducting the same experiment without reflectors. Consequently, the variation in declination angle is very small.

During the experimental study, the ambient temperature, absorber plate temperature, pot water temperature, enclosure air temperature, the solar radiation intensity and the wind velocity have been measured. Temperature measurements have been made using standard Type-T copper constantan thermocouples of ± 0.1 °C accuracy. Wind velocity has been measured by a wind cup anemometer whose accuracy is ±0.1 m/s. The solar radiation intensity on horizontal surface has been measured using Eppley PSP pyranometer which has an accuracy of ±1.5%. All measuring transducers have been connected to a data acquisition system interfaced with a PC. Measurements have been recorded at 15 minutes intervals during the effective sunshine period of 10:00 AM to 16:00 PM and then averaged over one hour periods.

Observations of typical diurnal variations in the absorber plate (T_p), enclosure air (T_a) and pot water (T_w) temperatures of the cooker with 0.25, 0.5 and 1 liter of water in the cooking pot with and without reflector are presented in fig. 2. From the figure, it is seen that the temperatures of the cooker components increase with time of day until they reached their maximum values around solar noon at high solar radiation. The maximum temperature recorded for absorber

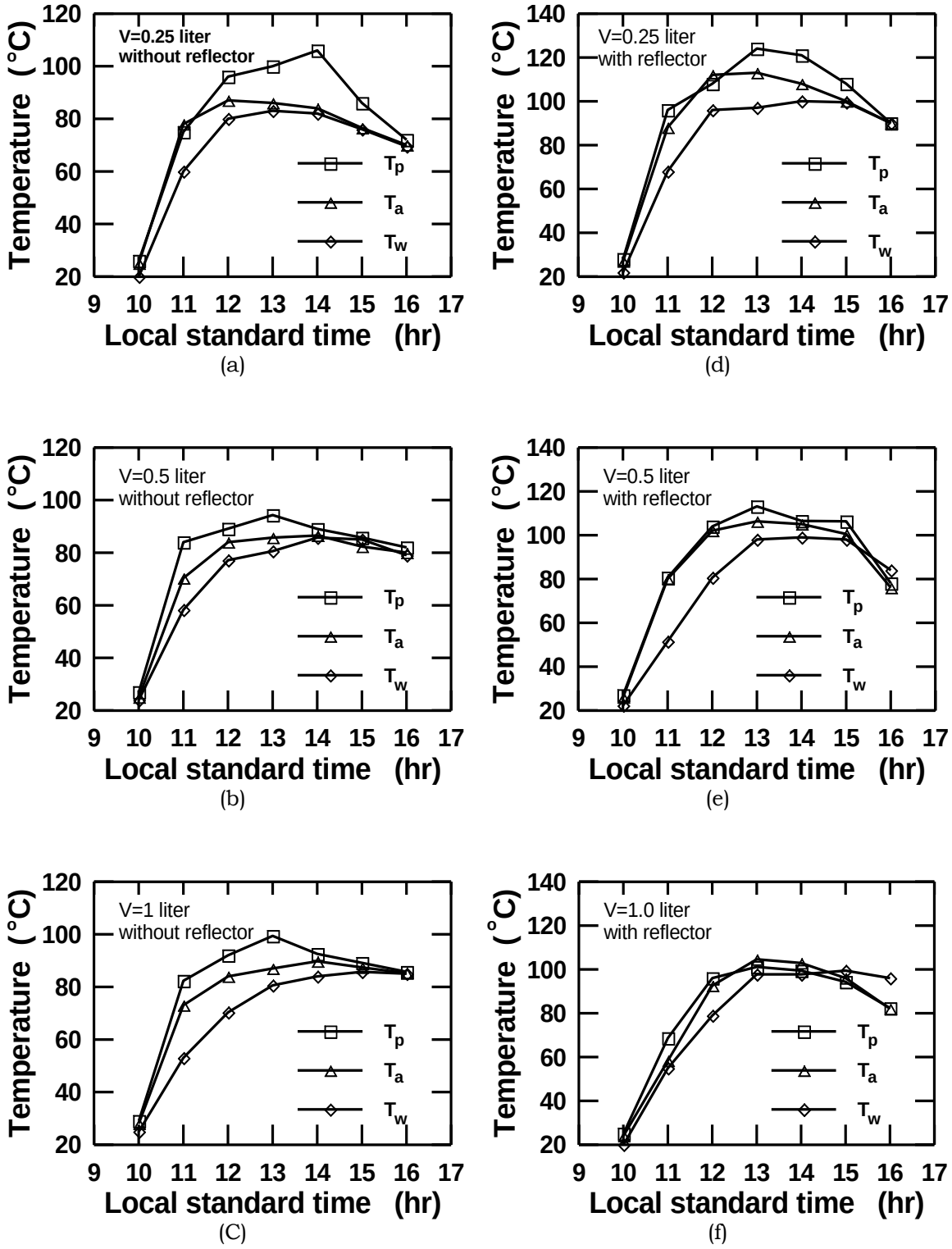

Fig. 2. Daily variation of plate, enclosure air and water temperatures for different quantities of water with and without reflectors.

plate, enclosure air, and pot water is 106, 89.7, and 85.7 °C respectively when no reflectors are used. The corresponding values measured with reflectors are 124, 113, and 99.4 °C respectively.

The daily thermal efficiency has been calculated to evaluate the performance of the cooker. The thermal efficiency of solar cooker, η_t, is the ratio between the energy required to raise the temperature of water from T_i to T_f and the amount of solar energy available for heating at the frontal area.

$$\eta_t = \frac{m_w C_w (T_f - T_i)}{I_G A_c \Delta\tau}. \quad (1)$$

Where $\Delta\tau$ is the time required to achieve the maximum temperature of the cooking water, A_c is the aperture area (m^2), m_w is the mass of water (kg), and I_G is the average solar radiation intensity (W/m^2).

The effects of using the reflectors and the quantity of water in the cooking pot on the thermal efficiency of the solar cooker are illustrated in fig. 3. It can be seen clearly that the thermal efficiency has remarkably increased with increasing the quantity of water in the cooking pot and with using reflectors. The thermal efficiency increases from 5.95 to 21.61 % as the quantity of water increases from 0.25 to 1 liter when no reflectors are used. The efficiency increases from 9.53 to 30.54 % by using reflectors. Therefore, the thermal performance of the cooker has been greatly improved by augmenting the radiation collection area using plane reflectors. This can be attributed to the shorter time taken water to get heated from the initial to the final temperature when the reflectors are used.

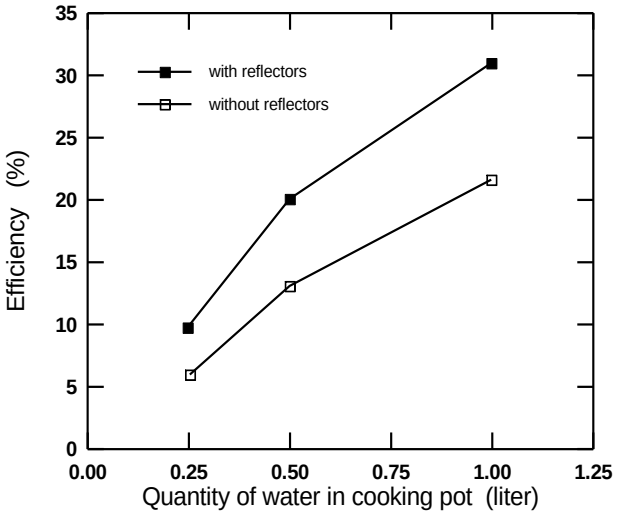

Fig. 3. Variation of cooker thermal efficiency with quantity of water in the cooking pot.

4. Artificial neural network principles

ANN are computational models based on the information processing system of the human brain. In general, it is composed of three layers; an input layer, some hidden layers and an output layer. Each layer has a certain number of small individual and highly interconnected processing elements called neurons or nodes. The neurons are connected to each other by communication links that are associated with connection weights. Signals are passed between neurons over the connection weights. Each neuron receives multiple inputs from other neurons in proportion to their connection weights and generates output signals which may be propagated to other neurons [13 and 15].

To develop an ANN model, the network is processed through two stages: Training/ learning stage and testing/validation stage. In the training/learning stage, the network is trained to predict an output based on the input data. In the testing/validation stage, the network is tested to predict the desired output. It is also used to calculate different measures of error. The network training process is stopped when the testing/validation error is within a desired tolerance [16 and 17].

Training of the ANN is accomplished by adjusting connection weights and minimizing the error between the network output and the desired output. An algorithm has to be used to obtain the desired output and to adjust the connection weights. The Back Propagation (BP) algorithm is the most popular and extensively used algorithm to minimize the error for the training process. The BP training algorithm consists of two phases. The first phase is the feed forward pass and the second phase is a backward pass. During the feed forward pass, the processing of information is

propagated from the input layer to the output layer. In the backward pass, the difference between obtained network output value from feed forward process and desired output is compared with the prescribed difference tolerance and the error in the output layer is computed. This obtained error is propagated backwards to the input layer in order to update the connection [12, 13 and 18].

Information processing of a neuron is illustrated in fig. 4. The input layer of network consists of (n) inputs and the hidden layer consists of (m) outputs (usually known as inputs of output layer) and output layer has only one output.

Each neuron of the input layer receives an input signal (x_i, i=1, 2,..., n) and broadcasts this signal to each neuron in the hidden layer. The input signal (net_j) for each neuron in the hidden layer is the sum of each input signal (x_i) multiplied by their corresponding weight (w_{ij}).

$$net_j = \sum_{i=1}^{n} x_i w_{ij} . \quad (2)$$

Then, this sum of weighted input signals of each neuron in the hidden layer is transformed through an activation function to produce an output signal (y_j; j = 1, 2, ..., m), which may be passed on the other neurons as follows:

$$y_j = f(net_j) = f\left(\sum_{i=1}^{n} x_i w_{ij} \right). \quad (3)$$

The activation function used in the hidden layer is a logistic transfer function defined as,

$$f(z) = \frac{1}{1 + e^{-net_j}} . \quad (4)$$

The same procedure is applied to the hidden layer and the output layer. Each output signal of the hidden layer (y_j) broadcasts to each neuron in the output layer. Therefore, the input signal (net_k) for each neuron in the output layer is the sum of all output signals of the hidden layer (y_j), multiplied by the corresponding weight (w_{jk}), as follows:

$$net_k = \sum_{j=1}^{m} y_j w_{jk} . \quad (5)$$

The subscripts i, j, and k indicates the number of neurons in the input, hidden and output layers, respectively.

Then, each neuron in the output layer applies an activation function to the sum of weighted input signal passing to the output layer in order to produce its final output signal.

$$O_k = f(net_k) = f\left(\sum_{j=1}^{m} y_j w_{jk} \right). \quad (6)$$

The activation function used in the output layer is same as in the hidden layer as follows:

$$f(z) = \frac{1}{1 + e^{-net_k}} . \quad (7)$$

Where net_k is the weighted sum of inputs to the k th neuron [16 and 17].

The BP training algorithm is a gradient descent algorithm that tries to improve the performance of the network and minimize the total error by changing the weights along its gradient. In other words, the BP training algorithm is a backwards processing of the error. It determines how closely the network output matches the desired output. The network output values are compared to actual values, if there is any difference, the connection weights are adjusted in a direction such that the error is decreased. This adjustment of the connection weights (w_{ij} and w_{jk}) is done iteratively by using the steepest gradient descent and it is propagated backwards from the output layer to the input layer. The error between network output and actual values is an indication of how successful the training is done. The performance of the network can be improved by minimizing the error with modifying the weights along its gradient. To start the training of the network, the initial connection weight values are chosen randomly. Then all

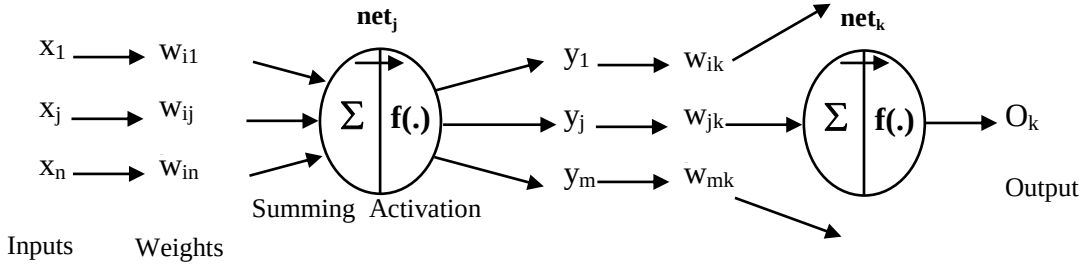

Fig. 4. The function of a single neuron.

weight values are initialized to training algorithm for beginning of training/learning process. As a result of the training or learning process the best weight values are produced. The weights contain meaningful information whereas before training they are random and have no meaning [11].

Training is halted when the value of the Sum of Squared Errors (SSE) has stopped decreasing and started to increase, which is an indication of over training. The prediction performances of the network is evaluated using the SSE, the statistical coefficient of multiple determination or correlation coefficients (R^2), and Mean Relative Error (MRE) values, which were calculated following expressions:

$$SSE = \sum_{k=1}^{n} (d_k - O_k)^2 . \quad (8)$$

$$R^2 = 1 - \frac{SSE}{\sum_{k=1}^{n} O_k^2} . \quad (9)$$

$$MRE(\%) = \frac{1}{n} \sum_{k=1}^{n} \left(\frac{|d_k - O_k|}{d_k} \right) \times 100 . \quad (10)$$

Where d_k is the desired or actual value, O_k is the network output or predicted value, and n is the number of output data [17].

5. Application of the ANN to experimental data

The objective of the developed ANN is to predict the absorber plate, enclosure air, and pot water temperatures of the solar cooker based on the solar radiation intensity, ambient temperature, time of day, quantity of water in the cooking pot, and with or without reflectors. The available data set from the experimental study was divided into two sub sets, training/learning and testing/validation sets. The experimental data set consists of 126 values. The ANN model was trained using randomly selected 96 data records (accounting for 75% of the total data) while the remaining 30 data records (accounting for 25% of the total data) was utilized for testing/validation of the network performance.

The ANN parameter values such as learning rate, momentum coefficient and number of neurons in the hidden layer are chosen with respect to the minimum SSE. The feed forward neural network structure was used in this study, which included an input layer, a hidden layer and an output layer, as shown schematically in fig. 5. The number of neurons in the input layer is equal to the number of input parameters. The number of neurons in the output layer is equal to the number of output parameters. The number of neurons in the hidden layer depends on the number of input and output parameters and the size of training data set. The optimum number of the neurons in the hidden layer was determined by trying two different networks. One network has 10 neurons and the other has 15 neurons. It has been found out that 10 neurons in the hidden layer were efficient enough for the optimum structure of the ANN. Therefore, the developed ANN architecture has a 5-10-3 neurons configuration.

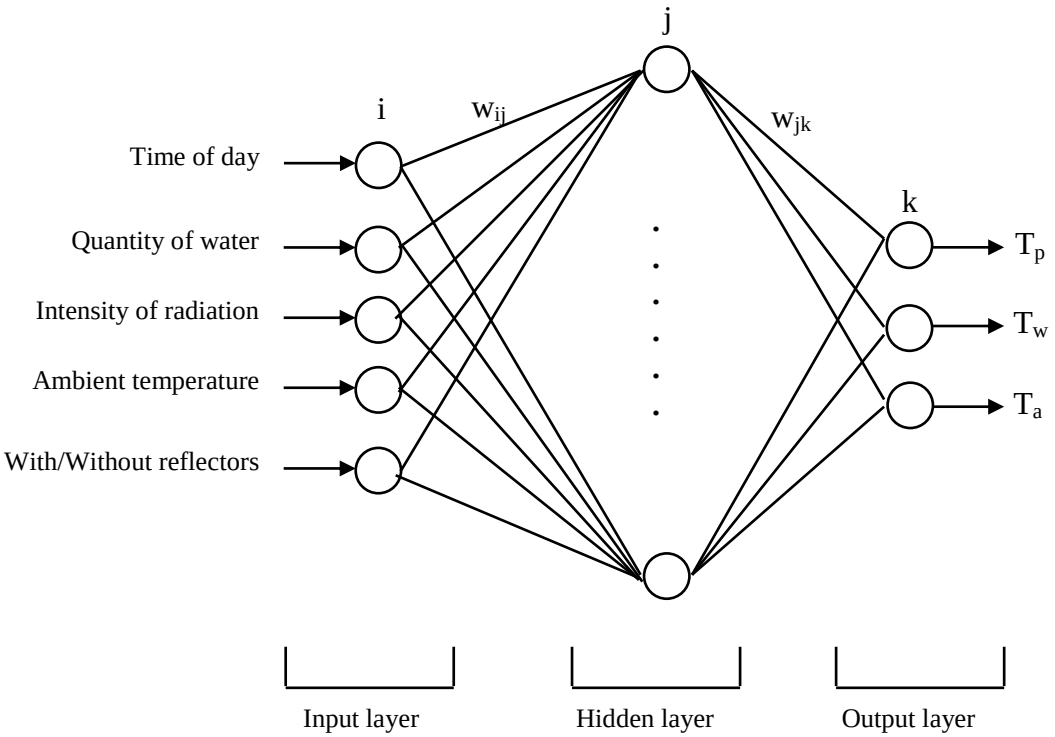

Fig. 5. The architecture of ANN used in this study.

After development of ANN architecture, the experimental data was normalized within the range 0.1 and 0.9 in order to improve training characteristics. Then normalized data was presented to the network as input data for training of the network. The back propagation algorithm was utilized in the training process. The connection weights were initialized randomly at the beginning of the training process. The network was trained until the error, which is defined as the sum of the squares of differences between desired output and network output, is acceptable. The SSE was chosen as 0.0004 in this study. If the SSE is greater than 0.0004, the network ran again through all the input data until the SSE was within the required tolerance. The prediction performances of the ANN were evaluated using MRE and correlation coefficient (R^2) value. A computer program was developed in visual basic to solve the proposed ANN model

6. Results and discussions

The predictions of the trained ANN for the absorber plate (T_p), enclosure air (T_a) and pot water (T_w) temperatures of the solar cooker with and without reflector for 0.25, 0.5 and 1 liters of water as a function of the experimental ones are shown in figs. 6 to 8 for training data set. To evaluate the accuracy of the ANN predictions, each graph is provided with a straight line indicating the perfect prediction. The performance of the neural network prediction was evaluated by regression analysis between the predicted and the experimentally measured values. The correlation coefficient (R^2) and mean relative error MRE of the regression analysis were considered as measures of prediction accuracy of the ANN model. The ANN predictions yield correlation coefficients in the range of 0.9979-0.9999 and MRE in the range of 0.271-1.56 %, as shown in the figures. The R^2 and MRE values are well within an acceptable range.

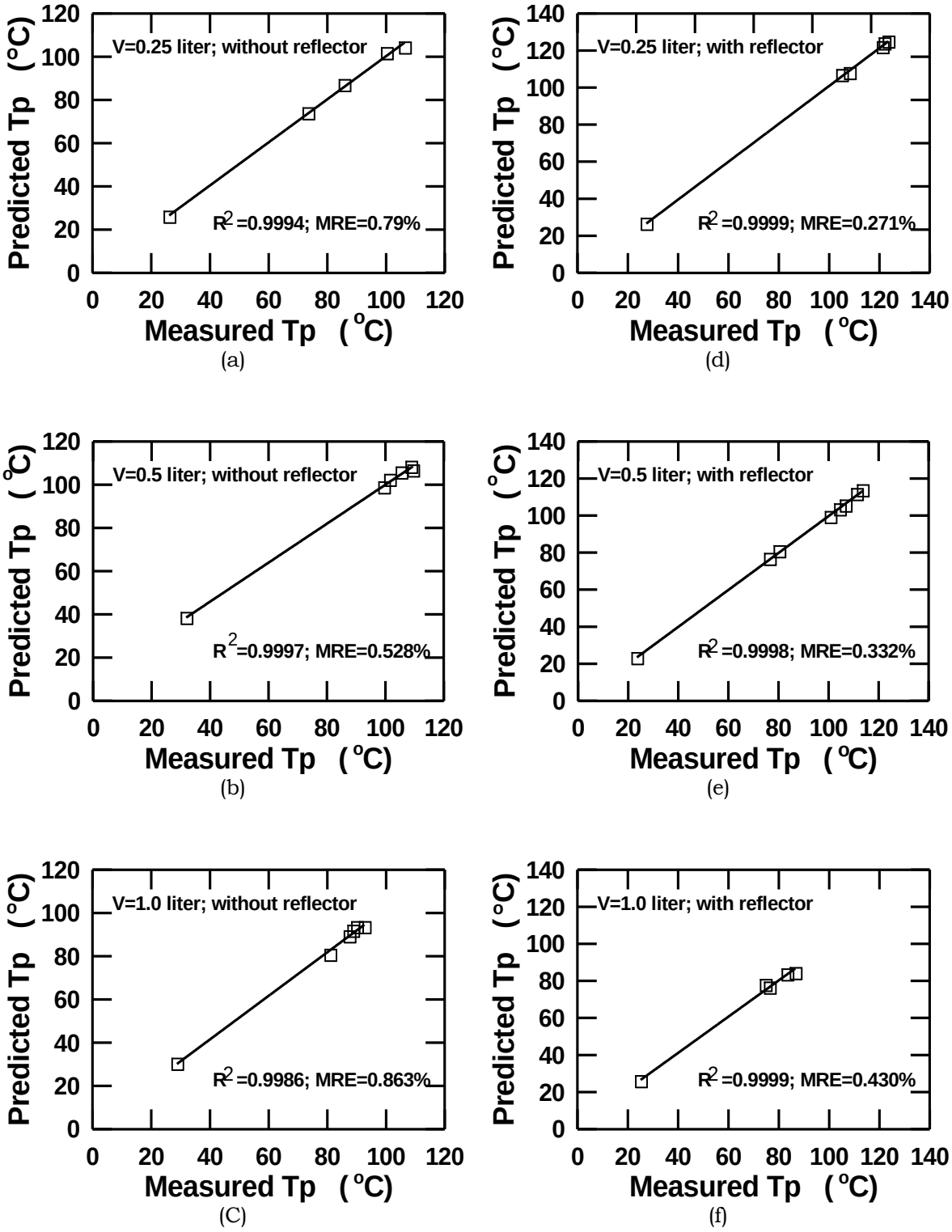

Fig. 6. Comparison of experimental measurements with predictions for absorber plate temperature using the training data set.

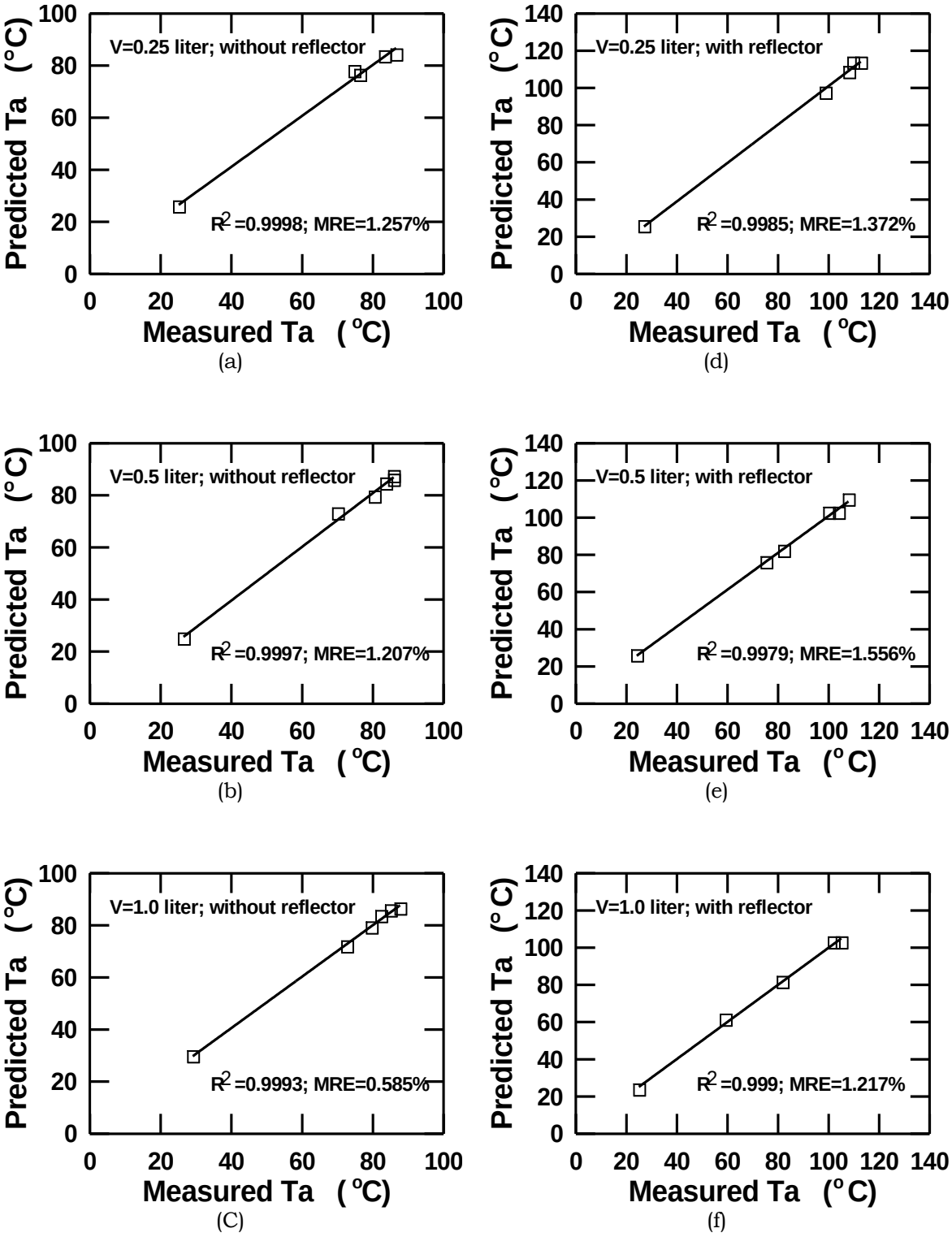

Fig. 7. Comparison of experimental measurements with predictions for enclosure air temperature using the training data set.

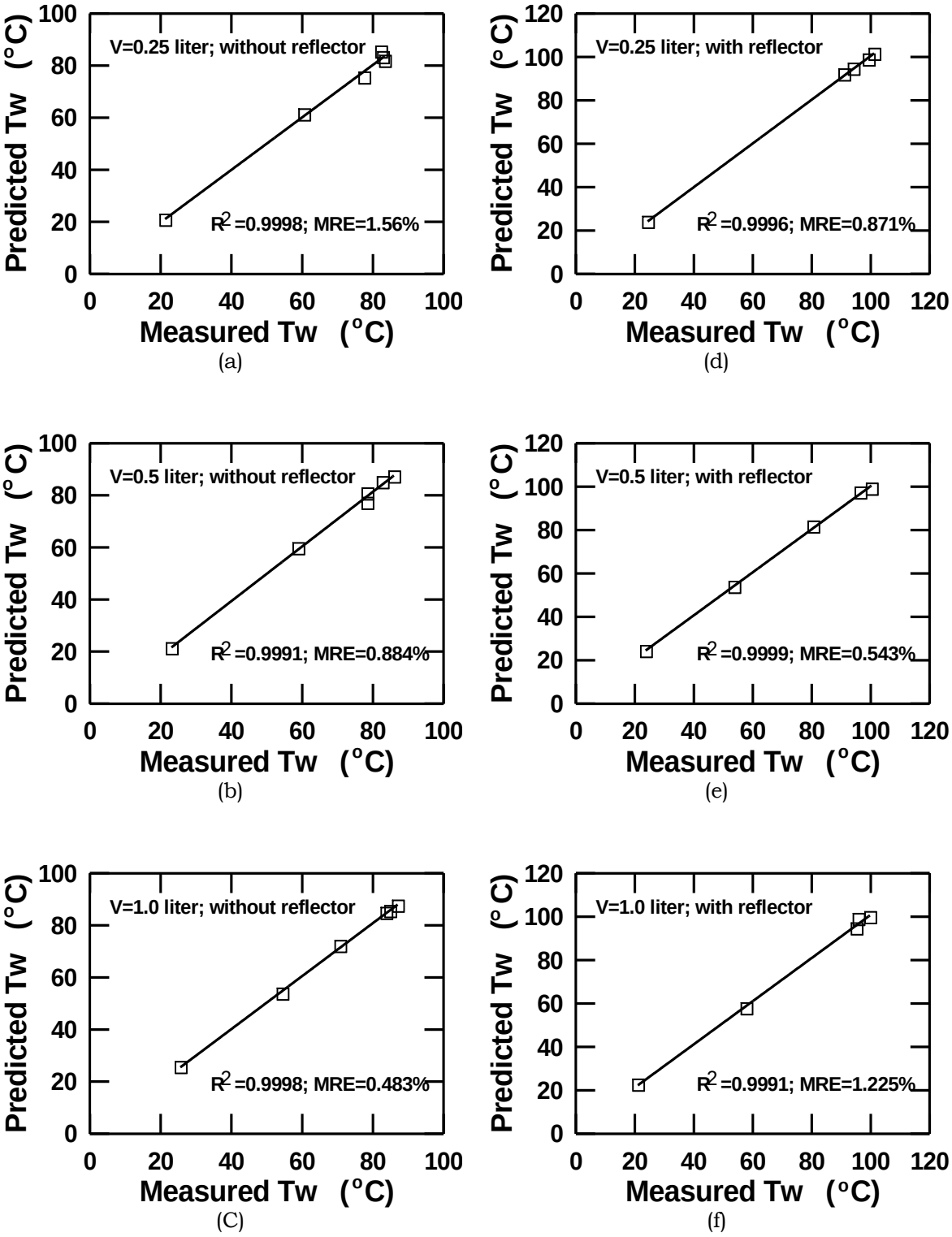

Fig. 8. Comparison of experimental measurements with predictions for pot water temperature using the training data set.

Therefore, these values show that the ANN predicts the absorber plate, enclosure air and pot water temperatures quite well.

A comparison of the ANN predicted values and experimentally measured values for temperatures for testing data set at with and without reflector conditions are given in figs. 9 and 10 respectively. Note that in these figures, the comparisons were made using only the values from the test data set, which was not introduced to the network during the training process and was selected randomly from experimental data set. The ANN predictions versus experimental values for the absorber plate, enclosure air and pot water temperatures without reflector are shown in fig. 9. The ANN prediction and experimental values for these temperatures yield correlation coefficients of 0.9982, 0.9973, and 0.9978 while the values of MRE are 6.411, 4.516, and 4.815 %, respectively. The ANN predictions for the absorber plate, enclosure air and pot water temperatures with reflectors as a function of the experimental values are shown in fig. 10. For predicting these temperatures with reflectors, the ANN yields correlation coefficients of 0.9823, 0.9942, and 0.9937 while the values of MRE are 6.751, 6.188, and 6.531 % respectively. Although the results obtained in case of using reflectors are poorer than those without reflectors, the regression coefficients obtained from testing the ANN were extremely good and well within acceptable limits in both cases. As the correlation coefficient approaches unity, the accuracy of the prediction improves. In the presented case, the correlation coefficients range is very close to 1, which indicates excellent agreement between the experimental and the ANN predicted results.

In order to assess the ANN thoroughly, comparisons with the results published in the literature have been made. The ANN has been applied to the systems described in references [4 and 6] and the predicted values have been compared with the results given in each reference. Fig. 11 shows a comparison between the ANN predictions and the theoretical estimations of plate temperature reported by Binark and Turkmen [4] using the second figure of merit F_2 during testing of a

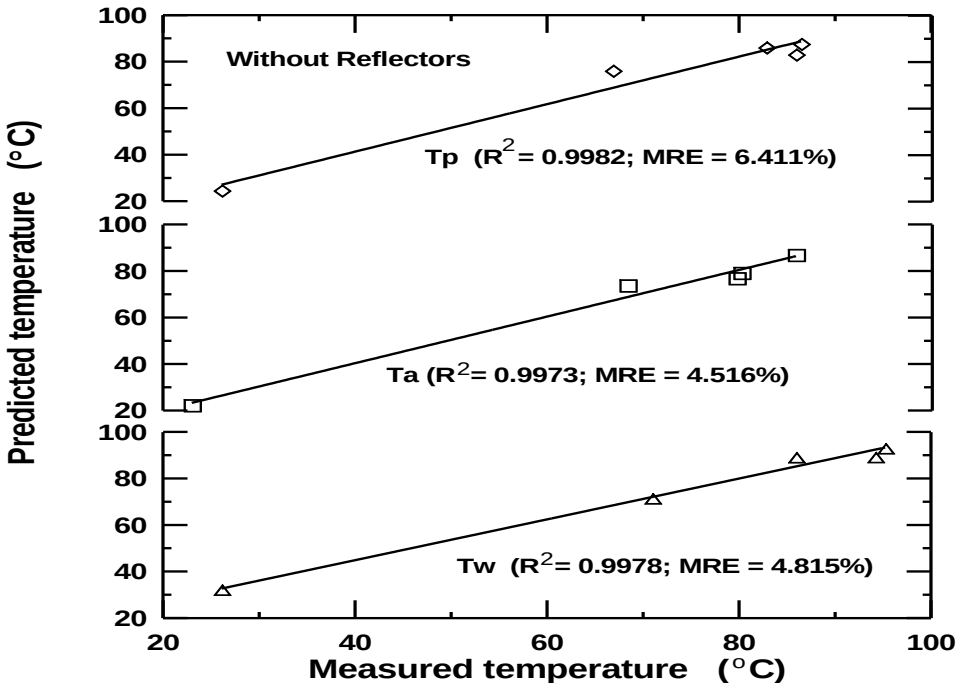

Fig. 9. Comparison of results between ANN predicted temperatures and measurements (without reflectors, test data set).

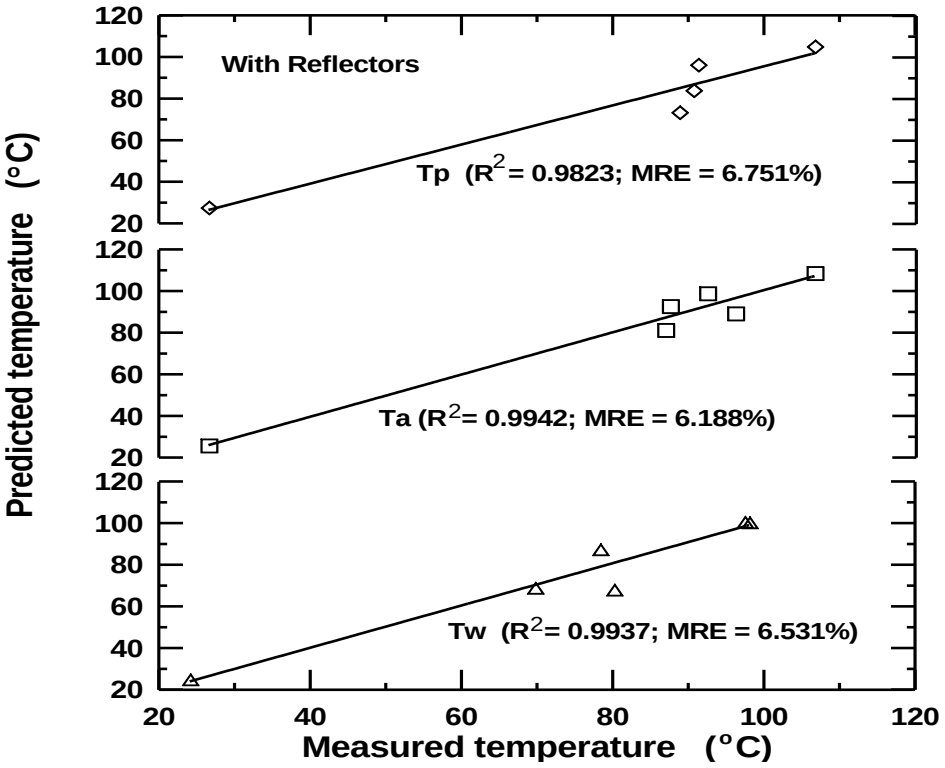

Fig. 10. Comparison of results between ANN predicted temperatures and measurements (with reflectors, test data set).

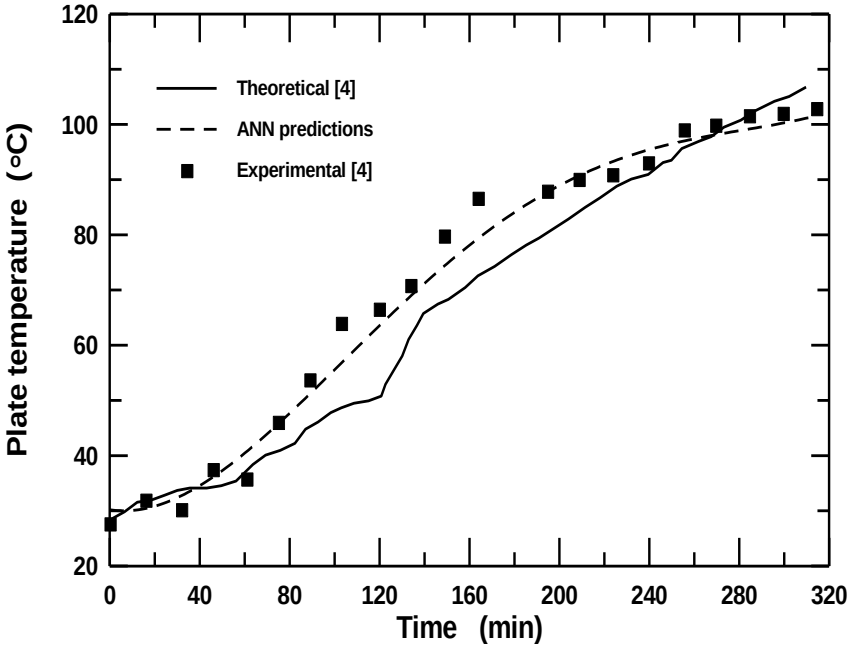

Fig. 11. Comparison of ANN predictions for plate temperature with previous work [4].

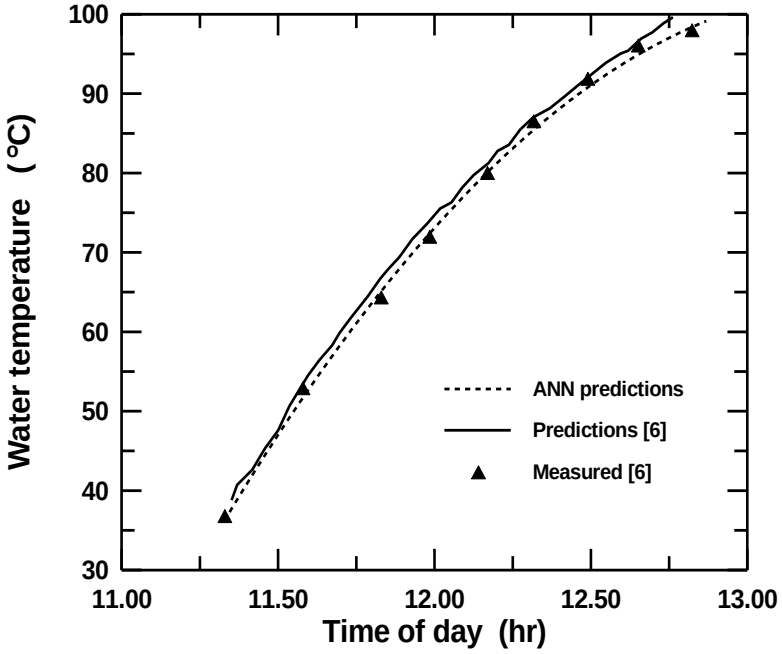

Fig. 12. Comparison of ANN predictions for pot water temperature with previous work [6].

cooker loaded by 3.5 liters of water. The experimental measurements reported in [4] are also shown in the figure. Another comparison has been also made with the theoretical results of Kumar [6] for pot water temperature using the fourth order Runge-Kutta method. This comparison is presented in fig. 12 along with the experimental measurements reported in [6] for a cooker containing 1 liter of water. A scrutiny of figs. 11 and 12 indicates that the agreement of predictions by the ANN with other models is quite reasonable. The closeness of ANN predictions to the measured values reveals also that the accuracy of the ANN is satisfactory.

7. Conclusions

This paper presents an application of the ANN in predicting the absorber plate, enclosure air and pot water temperatures of a box type solar cooker with and without reflectors for different quantities of water. The method uses solar radiation intensity, ambient temperature, quantity of water and time of day as inputs. An ANN model based on a back propagation algorithm was developed, which has a one hidden layer and 5-10-3 neurons configuration.

The prediction of performance using the ANN was compared with experimental measurements and their agreement was evaluated using the correlation coefficient (R^2) and MRE. The developed ANN model demonstrated a good regression analysis with the correlation coefficients in the range of 0.9823-0.9982 and MRE in the range of 4.516-6.751% for test data set. The regression coefficients indicated that the ANN approach could accurately be used as an alternative and practical technique to evaluate the thermal performance parameters of box type solar cookers.

References

[1] M. Grupp, P. Montagne and M. Wackernagel, "A Novel Advanced Box-Type Solar Cooker", Solar Energy, Vol. 47, pp. 107-113 (1991).

[2] N.M. Nahar, "Performance and Testing of a Hot Box Storage Solar Cooker", Energy Conversion and Management, Vol. 44 (8), pp. 1323-1331 (2003).

[3] E.H. Amer, "Theoretical and Experimental Assessment of a Double Exposure Solar Cooker", Energy

Conversion and Management, Vol. 44, pp. 2651-2663 (2003).
[4] A.K. Binark and N. Türkmen, "Modeling of a Hot Box Solar Cooker", Energy Conversion and Management, Vol. 37 (3), pp. 303-310 (1996).
[5] A.A. El-Sebaii, "Thermal Performance of a Box-Type Solar Cooker with Outer-Inner Reflectors", Energy, Vol. 22 (10), pp. 969-978 (1997).
[6] S. Kumar, "Estimation of Design Parameters for Thermal Performance Evaluation of Box-Type Solar Cooker", Renewable Energy, Vol. 30 (7), pp. 1117-1126 (2005).
[7] S.C. Mullick, T.C. Kandpal and S. Kumar, "Testing of Box Type Solar Cooker: Second Figure of Merit F_2 and its Variation with Load and Number of Pots", Solar Energy, Vol. 57 (5), pp. 409-413 (1996).
[8] P.A. Funk and D.L. Larson, "Parametric Model of Solar Cooker Performance", Solar Energy, Vol. 62 (1), pp. 63-68 (1998).
[9] A.A. El-Sebaii and A. Ibrahim, "Experimental Testing of a Box Type Solar Cooker Using the Standard Procedure of Cooking Power", Renewable Energy, Vol. 30, pp. 1861-1871 (2005).
[10] O.V. Ekechukwu and N.T. Ugwuoke, "Design and Measured Performance of a Plane Reflector Augmented Box-Type Solar-Energy Cooker", Renewable Energy, Vol. 28 (12), pp. 1935-1952 (2003).
[11] S.A. Kalogirou, "Artificial Neural Networks in the Renewable Energy Systems Applications: a Review", Renewable and Sustainable Energy Reviews, Vol. 5, pp. 373-401 (2001).
[12] N. Altinkok and R. Koker, "Mixture and Pore Volume Fraction Estimation in Al2O3/SiC Ceramic Cake Using Artificial Neural Networks", Materials and Design, Vol. 26, pp. 305- 311 (2005).
[13] J.S. Torrecilla L. Otero and P.D. Sanz, "Artificial Neural Networks: a Promising Tool to Design and Optimise High Pressure Food Processes", Journal of Food Engineering, Vol. 69 (3), pp. 299-306 (2005).
[14] J.A. Duffie and W.A. Beckman, Solar Engineering of Thermal Processes, Second Edition, John Wiley and sons Inc.; 1991.
[15] Y. Islamoglu, A. Kurt and C. Parmaksızoglu, "Performance Prediction for Non-Adiabatic Capillary Tube Suction Line Heat Exchanger: An Artificial Neural Network Approach", Energy Conversion and Management, Vol. 46, pp. 223-232 (2005).
[16] I.H. Yang, M.S. Yeo and K.W. Kim, "Application of Artificial Neural Network to Predict the Optimal Start Time for Heating System in Building", Energy Conversion and Management, Vol. 44, pp. 2791-2809 (2003).
[17] H. Kurt, K. Atik, M. Ozkaymak and A.K. Binark, "The Artificial Neural Networks Approach for Evaluation of Temperature and Density Profiles of Salt Gradient Solar Pond", Journal of the Energy Institute, (in press) (2006).
[18] G.E. Nasr and C.J. Badr, "Back-Propagation Neural Networks for Modeling Gasoline Consumption", Energy Conversion and Management, Vol. 44 (6), pp. 893-905 (2003).

Received September 28, 2006
Accepted January 31, 2007